*Environmental and Climate Technologies*

2019, vol. 23, no. 1, pp. 14–40
doi: 10.2478/rtuect-2019-0002
*https://content.sciendo.com*

# Application of Tropospheric Sulfate Aerosol Emissions to Mitigate Meteorological Phenomena with Extremely High Daily Temperatures

Gabriela C. MULENA[1–3]*, Salvador E. PULIAFITO[4, 5], Susan G. LAKKIS[6, 7]

[1]*Argentine Institute of Snow Research, Glaciology and Environmental Sciences (IANIGLA), Av. Ruiz Leal, Mendoza, Argentina*

[2,4]*Group of Atmospheric and Environmental Studies, Mendoza Regional Faculty, National Technological University, Rodriguez 273, Mendoza, Argentina*

[3,5]*National Scientific and Technical Research Council, Godoy Cruz 2290, Buenos Aires, Argentina*

[6] *Faculty of Engineering and Agricultural Sciences, the Pontifical Catholic University of Argentina, Av. Alicia Moreau de Justo 1300, Buenos Aires, Argentina*

[7]*Buenos Aires Regional Faculty, National Technological University, Medrano 951, Buenos Aires, Argentina*

***Abstract* – This research examined whether tropospheric sulfate ion aerosols ($SO_4^{2-}$) might be applied at a regional scale to mitigate meteorological phenomena with extremely high daily temperatures. The specific objectives of this work were: 1) to model the behaviour of $SO_4^{2-}$ aerosols in the troposphere and their influence on surface temperature and incident solar radiation, at a regional scale, using an appropriate online coupled mesoscale meteorology and chemistry model; 2) to determine the main engineering design parameters using tropospheric $SO_4^{2-}$ aerosols in order to artificially reduce the temperature and incoming radiation at surface during events of extremely high daily temperatures, and 3) to evaluate a preliminary technical proposal for the injection of regionally engineered tropospheric $SO_4^{2-}$ aerosols based on the integral anti-hail system of the Province of Mendoza. In order to accomplish these objectives, we used the Weather Research & Forecasting Model coupled with Chemistry (WRF/Chem) to model and evaluate the behaviour of tropospheric $SO_4^{2-}$ over the Province of Mendoza (Argentina) (PMA) on a clear sky day during a heat wave event occurred in January 2012. In addition, using WRF/Chem, we evaluated the potential reductions on surface temperature and incident shortwave radiation around the metropolitan area of Great Mendoza, PMA, based on an artificially designed aerosol layer and on observed meteorological parameters. The results demonstrated the ability of WRF/Chem to represent the behaviour of tropospheric $SO_4^{2-}$ aerosols at a regional scale and suggested that the inclusion of these aerosols in the atmosphere causes changes in the surface energy balance and, therefore, in the surface temperature and the regional atmospheric circulation. However, it became evident that, given the high rate of injection and the large amount of mass required for its practical implementation by means of the technology currently used by the anti-hail program, it is inefficient and energetically costly.**

***Keywords* – Integral anti-hail system of the Province of Mendoza; sulfate aerosols; weather modification; WRF/Chem**

* Corresponding author.
*E-mail address:* gmulena@mendoza-conicet.gob.ar

## 1. INTRODUCTION

Atmospheric aerosols play a key role in the climate system [1], [2]. They may influence the global radiation balance directly through the dispersion and absorption of the incident shortwave radiation (solar radiation) and the outgoing longwave radiation [3], [4], and semi-directly through changes in the structure of atmospheric temperature and in the evaporation rate of cloud droplets (i.e. fire cloud effect, [5], [6]). In addition, aerosols may affect the radiation balance indirectly through the alteration of the optical properties of clouds (i.e. the enhancement of cloud reflectance by increasing the total dispersion cross-sectional area, [7]) and the suppression [8], [9] or increase [10] of the precipitation regime.

Sulfate compounds are emitted into the atmosphere by natural sources (volcanoes, sulfur gases oxidation produced by plant decomposition) and also by anthropogenic sources, such as the combustion of sulfur containing fossil fuels, the smelting of ores and other industrial processes [11]. Anthropogenic and natural sources of sulfate aerosols are more abundant in the troposphere than in the stratosphere (Table 2 and Table 3, [12]). In addition to aerosol abundance, stratospheric and tropospheric aerosols also differ in lifetime. Sulfate aerosols can reside in the stratosphere for several months up to several years [13], and in the troposphere sulfate aerosols have a lifetime of a few weeks [14].

On the global perspective, tropospheric and stratospheric emissions of sulfate aerosols can affect the radiation budget of the Earth in two ways. Through the direct effect, they backscatter shortwave radiation and reduce the global mean surface air temperature (e.g., [15]). In this regard, estimates of direct forcing of tropospheric sulfate aerosols emitted from anthropogenic sources range from –0.3 to –0.9 W $m^{-2}$ [16]–[18]. Also, the stratospheric sulfate aerosol concentration due to strong eruptions, like 1991 Mount Pinatubo and 1982 El Chichon, have induced a negative radiative forcing [19], [20]: the Mount Pinatubo eruption was estimated to have contributed a maximum forcing of –4 W $m^{-2}$ and about –1 W $m^{-2}$ up to 2 years later, reducing the surface air temperature up to 0.5 °C [19]. Sulfate aerosols are hygroscopic having also an indirect effect, modifying cloud cover and cloud radiative properties (e.g., [21]). In this respect, the global mean indirect radiative impact from tropospheric sulfate in non-volcanic conditions has been estimated to be approximately –1.9 W $m^{-2}$ [22]. Likewise, aerosols injected into the stratosphere can reduce precipitation over land [23] and enter the troposphere through sedimentation or tropopause foldings and might affect cirrus clouds through aerosol-cloud interactions [24].

Several studies have shown that atmospheric aerosols may have a significant climatic impact at a tropospheric regional scale [1], [25]–[27]. Giorgi et al. and Qian and Giorgi [28]–[30] evaluated the regional climatic impact caused by anthropogenic sulfate aerosols in East Asia and found that they help explain the cooling observed in several regions for decades during the 20$^{th}$ century. Even more, Giorgi et al. [28] found that indirect aerosol effects induce a negative radiative forcing that results in a decrease of precipitation which prevails during the warm season. After that, Wu et al. [31] pointed out that the radiative forcing of sulfate aerosols was –0.39 W $m^{-2}$ over China. Ekman and Rodhe [32] conducted similar studies in Europe and found that anthropogenic industrial sulfate aerosols might cool the region by more than 1 °C.

Since atmospheric aerosols are capable of modifying the composition and behaviour of atmospheric dynamics, they can be used to artificially modify the weather or the climate. Aerosols have been used at a regional and urban scale to reduce hail [33], [34] and to improve or produce liquid precipitation or snow [35], [36], using silver iodide (Agl), lead iodide ($Pbl_2$), aluminum oxide ($Al_2O_3$) and barium (Ba) as seeding agents. At a global scale, an example of a theoretical intentional human intervention in the environment is the solar geoengineering method of injecting sulfate aerosols into the lower stratosphere, which have optical properties that allow the incoming solar

radiation to be dispersed [37], [38]. The method is based on the effects caused by sulfate emitted by large volcanic eruptions into the lower stratosphere, such as that of Mount Pinatubo in 1991 (e.g., [39], [40]). Solar geoengineering via aerosol injections aims at increasing sulfate aerosol levels, causing a rise in planetary albedo and diminishing the incoming solar radiation, thus reducing the mean global surface temperature (e.g., [41]). The discussion on the method has been mostly focused on the use of sulfur dioxide ($SO_2$). However, sulfate ion ($SO_4^{2-}$), hydrogen sulfide ($H_2S$), sulfuric acid ($H_2SO_4$), dimethyl sulfide (DMS), carbonyl sulfide (OCS), carbon sulfide ($CS_2$), ammonium sulfate ($(NH_4)2SO_4$) and engineered nanoparticles could also be used (e.g., [42]).

Some critical aspects in the design of the stratospheric sulfate injection plume such as the aerosol types, amount of spray injection, injection area, size distribution approach and injection rate and height have been discussed in geoengineering researches using general circulation models. In this respect, for example, stratospheric injection of $SO_2$ could be time-constant continuous (e.g., GeoMIP experiment G4, [43], [44]) or a time-varying (e.g., GeoMIP experiment G3, [44]); increasing amounts of $SO_2$ injections could be modified year by year to maintain the top-of-atmosphere net radiation constant (e.g., [45]). Since the resulting radiative forcing depends on both altitude and latitude of the geoengineering injection (e.g., [46]), $SO_2$ injection could be performed at several independent locations to obtain multiple climate objectives simultaneously [46], [47]; and $SO_2$ could be injected into seasonally varying areas to obtain more zonally uniform shortwave radiative forcing [48].

Most simulations of stratospheric aerosol geoengineering have focused in equatorial or tropical $SO_2$ injections (e.g., [44]). The use of sulfur dioxide is probably because of linear association between the size of $SO_2$ loading and the reduction in temperature evidenced in previous simulations (e.g., [49]). However, such simulations used a $SO_2$ size distribution based on observations of the eruption of Mount Pinatubo in 1991, which do not consider that the climatic effects of stratospheric injections could be limited by the increase of aerosols. In this regard, Heckendorn et al. [50] used a global model coupled with a two-dimensional aerosol microphysical model to simulate the nucleation, growth and coagulation of aerosols. Such modelling consisted of the injection of $SO_2$ at 50 hPa in a narrow region near the Equator, which showed that aerosols can grow more than twice their size compared to aerosols observed in Mount Pinatubo, and finally generate an aerosol particle with a shorter lifetime and less radiative forcing. In turn, Niemeier et al. [51] predicted that the injection of $SO_2$ at 30 hPa instead of 50 hPa increases aerosol loading by ~50 %. In order to increase loading and minimize the size of the sulfate aerosol, Pierce et al. [52] suggested using an injection of $H_2SO_4$ instead of $SO_2$ in a narrow region around the Equator. In addition, Pierce et al. found that the $H_2SO_4$ injection doubled the sulfate loading compared to the $SO_2$ injection used by Heckendorn et al. [50]. Vattioni et al. [53] corroborated previous study with uncoupled aerosol and radiation modules, suggesting that, compared to $SO_2$ injection, the direct emission of Accumulation-mode-$H_2SO_4$ droplet results in more radiative forcing for the same sulfur equivalent mass injection strength. English et al. [54] compared the efficiency of injecting three different kinds of sulfates: $SO_2$, $H_2SO_4$ and $SO_4^{2-}$. They found that the $SO_4^{2-}$ rather than the $SO_2$ injection increases sulfate loading, and that the $H_2SO_4$ injection rather than the $SO_2$ injection does not visibly alter the size or the mass of the sulfate, in contrast to the work conducted by Pierce et al. However, in line with the latter, they found that a $SO_4^{2-}$, rather than a $SO_2$ injection, with a log-normal distribution, a 1.5 width and a maximum radius peak of 0.1 μm, results in smaller particles and produces a mass loading 51 % higher than $SO_2$ in a narrow region located between 4° N and 4° S. Additionally, Visioni et al. [55] stressed that two global-scale models using different aerosol schemes (i.e. bulk and sectional schemes) can produce different results on the stratospheric sulfate lifetime and surface deposition, showing that it is still necessary to deepen into the subject.

The use of sulfate on a global scale is not the only possible deployment scenario, and specific consideration has been given to its use in tackling heat waves. In this regard, Bernstein et al. [56] showed the potential to mitigate a heat wave in a modelling case study with a regional chemical/dynamical model applying stratospheric sulfate injections. They studied the effect of regional-scale sulfate aerosol emissions over California during a two-day heat wave in July 2006 in order to quantify potential reductions in surface temperature. They found that for emission rates of approximately 30 $\mu g\ m^{-2}\ s^{-1}$ of sulfate aerosols at 12 km, produces temperature decreases of around 7 °C during the middle part of the day over the Central Valley; while metropolitan and regions affected by oceanic air showed slightly smaller reductions. The size and injection of the aerosols close to the target region raise substantial concerns.

The scope of this research work was to examine whether $SO_4^{2-}$ aerosols, considered at a global scale by solar geoengineering, might be applied at the tropospheric regional scale in order to mitigate meteorological phenomena with extremely high daily temperatures. Therefore, we listed the following specific objectives:

1) to model the behaviour of $SO_4^{2-}$ aerosols in the troposphere and their influence on temperature and surface incident solar radiation, using an appropriate online coupled mesoscale meteorology and chemistry model;

2) to determine the main geoengineering design parameters using tropospheric $SO_4^{2-}$ aerosols in order to artificially reduce the 2 m air temperature by 0.5 °C and the surface incident radiation during events with extremely high daily temperatures;

3) to evaluate a preliminary technical proposal for the injection of regionally engineered tropospheric $SO_4^{2-}$ aerosols.

Therefore, we used the Weather Research & Forecasting Model coupled with Chemistry (WRF/Chem: [57], [58]) to model and evaluate the behaviour of tropospheric $SO_4^{2-}$ at a regional scale over the Province of Mendoza (Argentina) during a heat wave event that occurred in January 2012. In addition, using WRF/Chem, we evaluated the potential reductions in temperature and surface incident shortwave radiation around the metropolitan area of Great Mendoza, Province of Mendoza, based on an artificially designed aerosol layer and on observed meteorological parameters. In this work, we sought to implement $SO_4^{2-}$ seeding using the technological infrastructure currently used by the operational anti-hail program of the Province of Mendoza [34], [59].

## 2. METHODS AND PROCEDURES

### *2.1. Case Study*

Heat waves are usually associated with quasi-stationary anomalies in atmospheric circulation that produce subsidence, weak winds, clear skies, adiabatic warming, warm air advection, positive anomalies in incident solar radiation as a result of the reduction in cloudiness and prolonged heat conditions on the surface. Various regions on the planet have already experienced the effects of these events, resulting in mortality and morbidity in thousands of people [60]. Furthermore, heat waves have an impact on agricultural resources, on industry and tourism [61], and on ecology [62]. They increase the demand for water and energy [63]; and the risk of forest fires [64] and droughts [65], in addition to facilitating the photochemical production of contaminants such as ozone, the emission of biogenic isoprene organic compounds and the production of secondary aerosols such as peroxyacetyl nitrate [66]. In South America and Argentina, heat waves have been extensively investigated [67], [68].

The Province of Mendoza, located in the southwest of the Argentine Republic, has been frequently affected by heat waves [69]. In this aspect, in the province, a heat wave is declared when the

minimum daily temperature at 2 m does not drop below 20 °C for at least 3 consecutive days. January 2012 was no exception since a heat wave was registered which increased power consumption in the region and the number of people affected by heat stroke [70].

In this work, we focused our studies on the urban metropolitan area of Great Mendoza (32° 47' 59.1" S – 33° 02' 34" S, 68° 53' 59.5" W – 68° 36' 57.1" W, 750 m a.s.l., total surface area of 170 km$^2$) of the Province of Mendoza on January 8, 2012, since that date exhibited favourable meteorological conditions for injecting $SO_4^{2-}$ aerosols in the troposphere in a clear sky and, therefore, for analysing the direct effects of such aerosols (Fig. 1). The analysed urban center is located in the North Center of the province, in the piedmont of Los Andes Mountain Range [71].

Below, we present the atmospheric patterns associated to the month of January 2012 and, in particular, those corresponding to January 8.

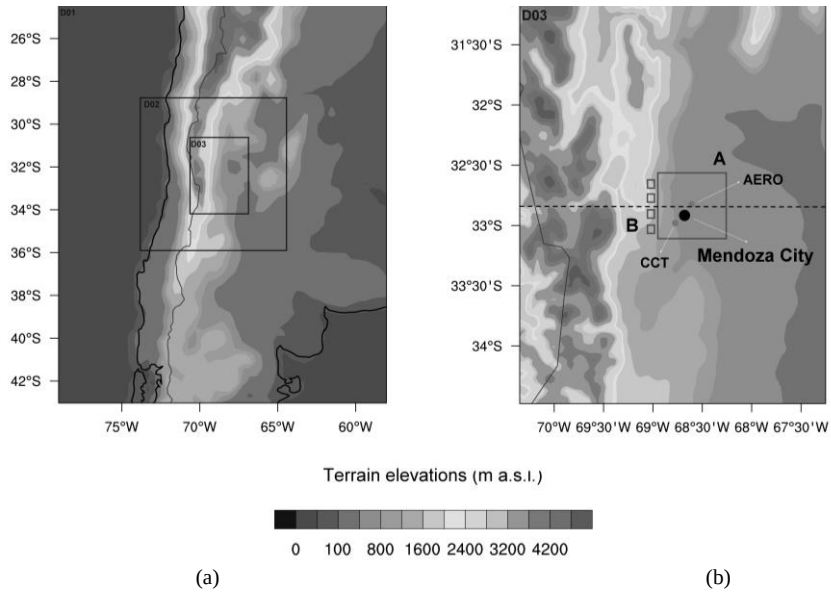


Fig. 1. Province of Mendoza, located in Western Argentina, and metropolitan area of Great Mendoza, located in the center-east of the Province of Mendoza: a) WRF/Chem-modelled nested domains, with the terrain heights in m a.s.l.: Domain D01 (36-km horizontal spatial resolution), Domain D02 (12-km horizontal spatial resolution), Domain D03 (4-km horizontal spatial resolution); b) Domain D03 enlarged, together with the distribution of the emission sources of tropospheric $SO_4^{2-}$ aerosols, according to configurations A and B. The black dot shows the location of the City of Mendoza (32° 54' S, 68° 51' W). The grey dots indicate the CCT (32° 53' S, 68° 52' W) and AERO (32° 50' S, 68°48' W) weather stations. Dotted line: cross-sectional cut.

### *2.1.1. Atmospheric Conditions on January 8, 2012*

Fig. 2 shows the compositions of the surface temperature anomalies at 1000 hPa and the evolution of outgoing longwave radiation anomalies at the top of the atmosphere on January 8, 2012. That day exhibits a stationary center of strong positive anomalies located at approximately 40° S 67° W and positive anomalies in longwave radiation associated to lower convection activity covering practically the entire Argentine territory.

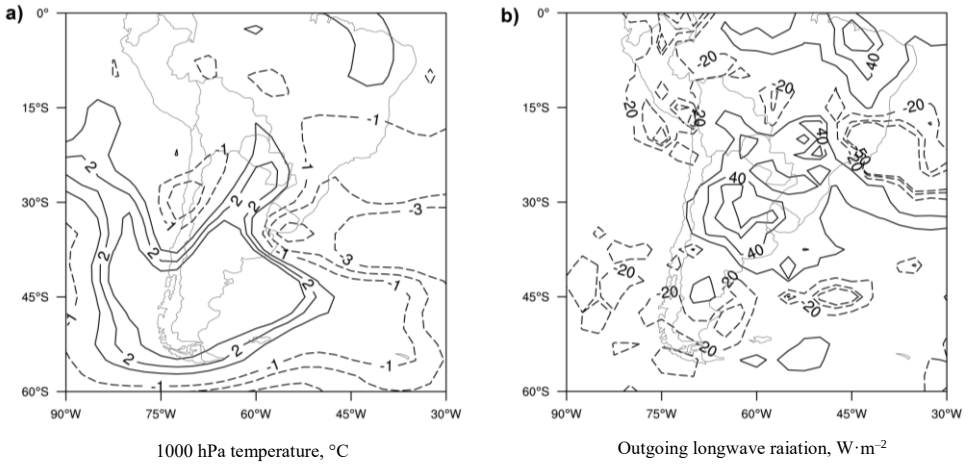


Fig. 2. Composites anomalies of: a) 1000 hPa temperature; b) outgoing longwave radiation at the top of the atmosphere, for 8 January 2012 and the climatological mean of the 1981–2010 interval. Figure built from images provided by the Earth System Research Laboratory of the National Oceanic and Atmospheric Administration, Boulder, Colorado, on its website [72].

In turn, Fig. 3 shows the air temperature at 2 m for the same day, recorded at the surface meteorological station of the Argentine Council of Scientific and Technical Research – Mendoza (CCT) (32° 53' S, 68° 52' W) and Mendoza International Airport (AERO) (32° 50' S, 68° 48' W). According to the image, the 2 m air temperature on that day at both stations reached its minimum value (21–22 °C) around 8:00 LT. After 9:00 LT, it started to rise until 20:00 LT, when it started to drop again. Therefore, the meteorological intervention of injecting tropospheric $SO_4^{2-}$ aerosols took place between 9:00 and 20:00 LT.

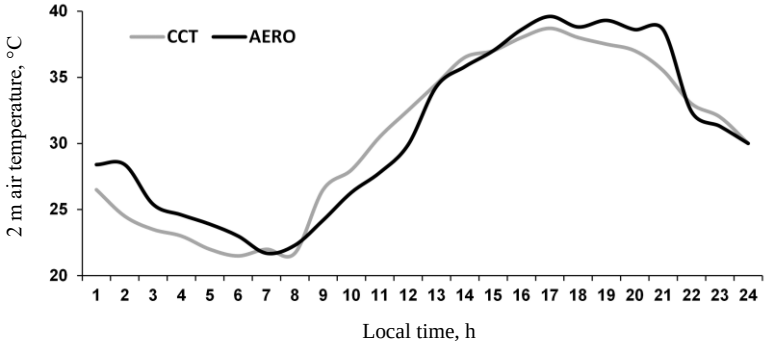


Fig. 3. 2 m air temperature at CCT (32° 53' S, 68° 52' W) and AERO (32° 50' S, 68° 48' W) surface meteorological stations for 8 January 2012.

Fig. 4 shows the radiosounding for 8 January 2012 at 9:00 LT. The air temperature curve observed indicates that the air layer located at around 600 hPa (~ 4 km a.s.l.) and 850 hPa (~2 km a.s.l.) has a positive atmospheric stability. This situation determines that the rise of an artificial sulfate injection will be limited by the stability of those two layers. The air temperature and

wind speed at 850 hPa reach 19 °C and 18 km $h^{-1}$, respectively. At 600 hPa, air temperature is 4.6 °C and wind speed 40 km $h^{-1}$. Moreover, winds blow from the northwest in both pressure levels. In addition, surface air temperature is 24 °C and 10 m – wind speed is 3.7 km $h^{-1}$, coming from the south.

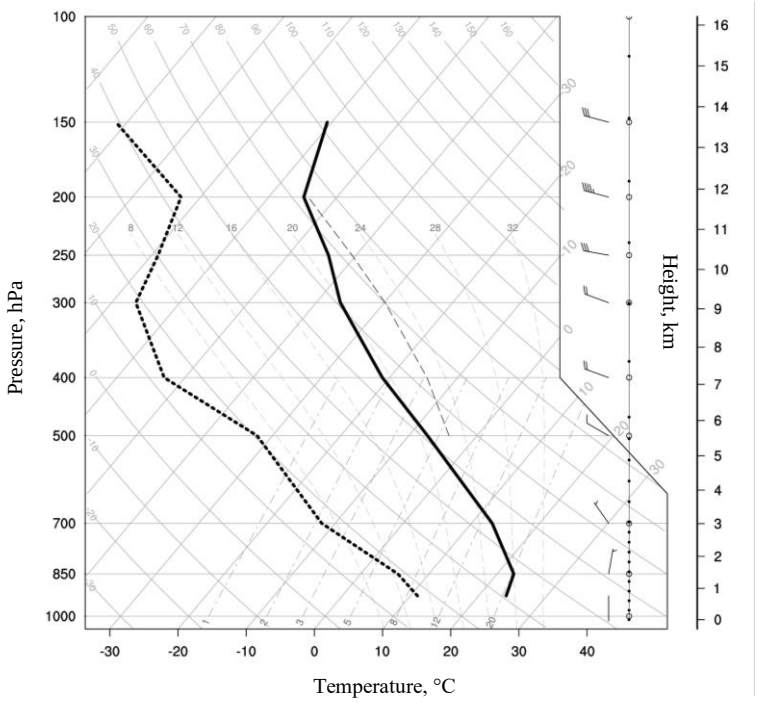


Fig. 4. Radiosounding observed at the AERO meteorological station (32° 50' S, 68° 48' W) for 8 January 2012 at 9:00 LT.

For 8 January 2012, at a regional scale, Fig. 5 indicates that the mean wind speed around 32° S – 68° W is around between 40 and 60 km $h^{-1}$ at 850 and 600 hPa, respectively. At both pressure levels, the average wind direction comes from the north-northwest. Additionally, Fig. 6 shows that the average daily thermal gradients around the same point have an absolute thermal stability at 850 and 600 hPa.

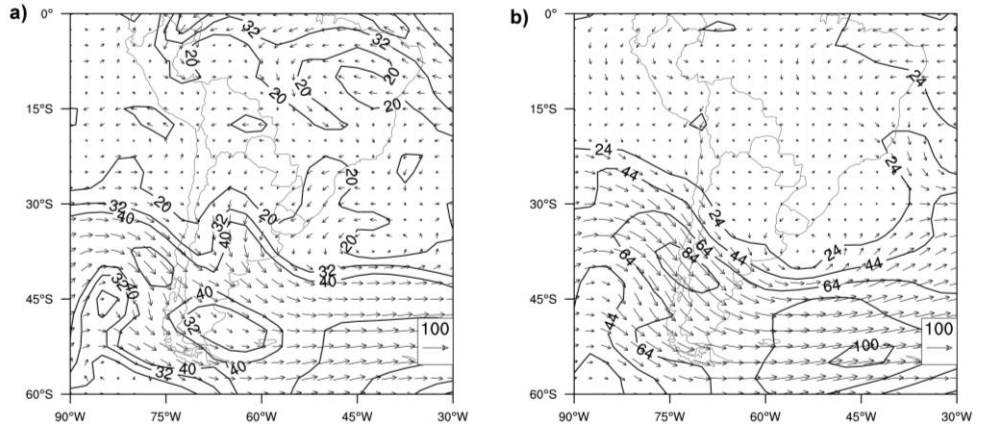


Fig. 5. Average wind speed (contour) and direction (arrows) for 8 January 2012 at: a) 850 hPa; b) 600 hPa. Figure built from images provided by the Earth System Research Laboratory of the National Oceanic and Atmospheric Administration, Boulder, Colorado, on its website [72].

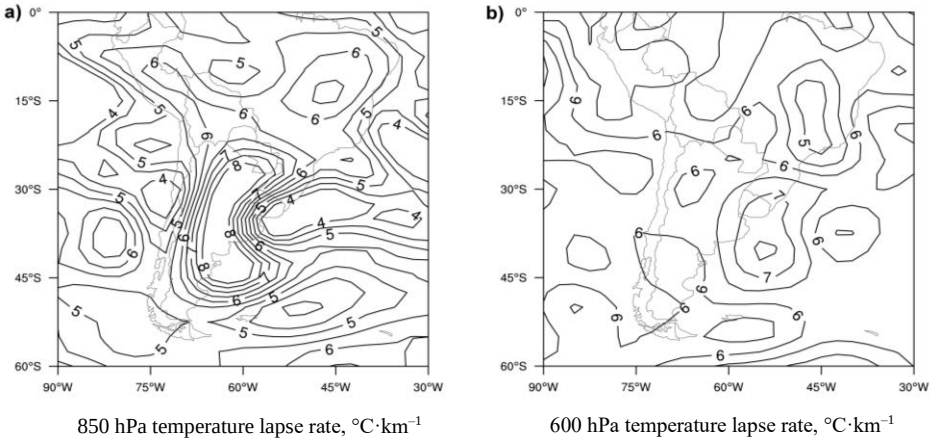


Fig. 6. Average thermal gradient for 8 January 2012 at: a) 850 hPa; b) 600 hPa. Figure built from images provided by the Earth System Research Laboratory of the National Oceanic and Atmospheric Administration, Boulder, Colorado, on its website [72].

Analysing the data from the Global Forecast System (GFS: [73]), it can be observed that on January 8 2012 between 9:00 and 20:00 LT, the winds of both stable layers came from the north and north-east (figures not shown here).

### *2.1.2. Design and Control of the Tropospheric Sulfate Aerosol Emissions in the Study Area*

In this research study, we simulated the seeding of $SO_4^{2-}$ based on the technological infrastructure currently used by the operational anti-hail program of the Province of Mendoza [34]. The seeding system has two Agl injection methods. The first one consists of the use of four Cheyenne turboprop aircraft, which use two types of explosives (cartridges and flares). The second method consists of

using more than a dozen surface generators which emit Agl with dissolution of acetone, located in areas where air operations are restricted.

The simulated sulfate emissions were controlled by:

1) meteorological parameters;
2) target area;
3) and the sulfate emission source.

In this context, the most significant meteorological parameters considered in the design for the injection of tropospheric $SO_4^{2-}$ aerosols were: wind speed, direction and persistence, longwave radiation at the top of the atmosphere, and atmospheric thermal stability, the latter being determined by calculating the temperature difference between an air parcel and the surrounding air. In addition, the target area, that is, the site where the impact of the tropospheric $SO_4^{2-}$ aerosols applied at a regional scale is to be evaluated, was Great Mendoza (32° 50' S, 68° 50' W, 750 m a.s.l.).

In turn, the emission source was described by the emission height, the distribution of the emission sources, rate (period) of injection and emission rate.

The maximum height of $SO_4^{2-}$ emission is found at 600 hPa (4 km a.s.l.), that is, in the atmospheric layer of no divergence, no convergence, maximum vertical speed or maximum rise or fall. In turn, the minimum height of aerosol emissions was at the upper limit of the planetary boundary layer located in the City of Mendoza (32° 54' S, 68° 51' W) at 850 hPa, between 1.5 and 2 km a.s.l. The stratosphere layer has not been considered a desirable injection level since it is dominated by fast westerly wind speeds (~80 km $h^{-1}$) which may reduce the sulfate lifetime over the Province of Mendoza during heat waves (see Fig. 7).

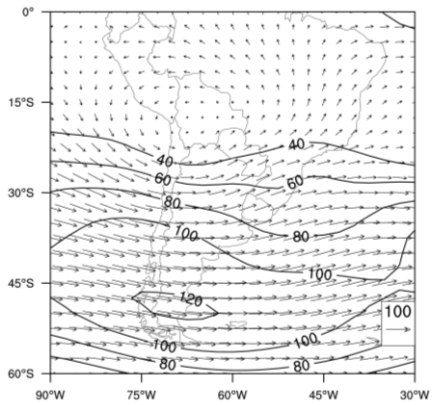


Fig. 7. Average wind speed (contour) and direction (arrows) at 200 hPa for three-day heat waves during the summer period of the years 1977–2018 in the Province of Mendoza. Figure built from images provided by the Earth System Research Laboratory of the National Oceanic and Atmospheric Administration, Boulder, Colorado, on its website [72].

For this experiment, we proposed several distribution schemes for the emission sources. According to the analysis of $SO_4^{2-}$ aerosol lifetime in the troposphere, we established two injection methods: continuous and pulsating.

The minimum injection rate was set at 100 g $s^{-1}$ per $km^2$, considering the maximum industrial emission rates of Argentina. In this work, we also considered other lower rates (30 and

50 g $s^{-1}$). The maximum emission rate was determined at 1000 g $s^{-1}$ per $km^2$, based on industrial emissions derived from mega cities such as Mexico [74].

### *2.2. Modeling System Used in the Injection of Tropospheric Sulfate Aerosols*

Studies on the impact of the tropospheric injection of $SO_4^{2-}$ at a regional scale require accurate models which include the interactions between air contaminants and meteorological conditions. In order to design the injection of tropospheric $SO_4^{2-}$, in this work we used version 3.5 of the WRF/Chem model. WRF/Chem is an online model used in many previous studies (e.g., [75], [76]), with a modular structure capable of considering a variety of physical and chemical processes simultaneously coupled with meteorology, such as transport, mixture, deposition, emission, chemical transformation, aerosol interactions, photolysis processes and radiative transfer [57]. The short chemical time steps used by WRF/Chem make it a suitable model to study short lifetime species (<5 days), such as tropospheric $SO_4^{2-}$.

The chemical simulations of the regional design for tropospheric injections of $SO_4^{2-}$ with WRF/Chem were configured with 3 nested domains with a 3:1 ratio using the 1-way nesting strategy (Table 1). This type of nesting allows the finer resolution domain to acquire the initial and boundary chemical conditions of its preceding domain. In this way, we obtained two more external domains with a horizontal spatial resolution of 36 km (D01) and 12 km (D02), approximately centered at 32° S 68° 30' W, and an internal domain of 4 km (D03) centered in the City of Mendoza. Domains D01, D02 and D03 covered a total surface area of approximately 4 000 000, 650 000 and 105 000 $km^2$, respectively. The simulations performed with the design covered 15 days of simulation, from 1 January 2012 at 0 UTC to 15 January 2012 at 0 UTC.

TABLE 1. LOCAL CONFIGURATION OF WRF/CHEM (MULENA ET AL. [77] AND GRELL ET AL. [57] AND INTERNAL REFERENCES)

| Parametrization | Schemes | D01 | D02 | D03 |
|---|---|---|---|---|
| Input | | | | |
| Terrain elevation | SRTM3[1] | – | – | – |
| Land Use-Land Cover | Customized | – | – | – |
| Analysis | GFS[2] 0.5 · 0.5 | | | |
| Resolution | | | | |
| Temporal | Δt (seg) | 216 | 180 | 24 |
| Spatial | Δx, Δy (km) | 36 | 12 | 4 |
| Vertical | Δη (ETA levels) | 40 | 40 | 40 |
| Upper pressure | p_top (hPa) | 50 | 50 | 50 |
| Dynamics | | | | |
| Integration | 2nd order Runge-Kutta | 3 | 3 | 3 |
| Vertical speed | Damping enabled | 1 | 1 | 1 |
| Turbulence and mixture | 2nd order diffusion | 1 | 1 | 1 |
| Eddy Coefficients | Smagorinsky | 4 | 4 | 4 |
| Horizontal scalar advection (vertical) | – | 5 | 5 | 5 |
| Horizontal moment advection (vertical) | – | 5 | 5 | 5 |
| Prognosis | Enabled | 0 | 0 | 0 |
| Physical parametrizations | | | | |
| Microphysics | Morrison's two moments | 10 | 10 | 10 |

| | | | | |
|---|---|---|---|---|
| Longwave radiation (LW) | RRTM[3] | 1 | 1 | 1 |
| Shortwave radiation (SW) | Goddard | 2 | 2 | 2 |
| Soil | Noah Land Surface Model | 2 | 2 | 2 |
| Soil Surface levels | – | 4 | 4 | 4 |
| Physical surface layer | Monin-Obukhov Similarity Theory | 1 | 1 | 1 |
| Planetary boundary layer | YSU[4] | 1 | 1 | 1 |
| Cumulus | Kain-Fritsch scheme | 1 | 1 | 1 |

Note: 1. SRTM3: Shuttle Radar Topography Mission Data; 2. GFS: Global Forecast System [73]; 3. RRTM: Rapid Radiative Transfer long-wave Model; 4. YSU: Yonsei University.

Table 1 lists the WRF/Chem physical and dynamical parametrizations used. The grid nudging option of the WRF's Four-Dimensional Data Assimilation (FDDA) system was used in domain D01, as suggested by Carvalho et al. [78]. However, to avoid possible interferences in the resolved mesoscale forcing mechanisms that are important to the development of the boundary layer [79], no nudging was applied inside the Planetary Boundary Layer. Regarding the chemical parametrizations, all the simulations employed the gas-phase model known as Regional Acid Deposition Model 2 (RADM2: [80]) and the aerosol model, called Modal Aerosol Dynamics Model for Europe (MADE/SORGAM: [81]). The initial and boundary chemical conditions, that is, the chemical concentrations of aerosols and gas for domain D01 of the regional design are idealized. The inner domains in both designs obtain their chemical conditions from their parent domains: D02 from D01 and D03 from D02. Additionally, chemical emissions from aerosols and gases, derived from anthropogenic, natural and biogenic sources, were used. Biomass burning sources were disregarded. Anthropogenic chemical emissions for all domains derive from global databases: REanalysis of the TROpospheric chemical composition (RETRO: [82]) and Emission Database for Global Atmospheric Research (EDGAR: [83]). Both databases were modified using the chemical speciation of the emissions inventory of the National Emissions Inventory for the U.S.A. (NEI [84]). In addition, all the domains employ GOCART background emissions [85]. Biogenic emissions for all the domains derive from the Model of Emissions of Gases and Aerosols from Nature version 3.1 (MEGAN: [86]), and GOCART natural emissions [85].

The injections of $SO_4^{2-}$ into the troposphere and the tests on their impact were performed in domain D03. Seven experiments were conducted in this domain: one simulation without $SO_4^{2-}$ emissions called Test_Control and six simulations with $SO_4^{2-}$ emissions detailed in Table 2. The simulations with aerosol emissions included two types of $SO_4^{2-}$, the Aitken mode (SO4I) and the Accumulation mode (SO4J). Emission rates range between 30 and 1000 g $s^{-1}$ per $km^2$ and injection heights correspond to 2 and 4 km a.s.l. Note that injections begin at 8:00 LT (11:00 UTC). Table 2 shows two different types of source distributions of tropospheric $SO_4^{2-}$ that cover the target area: A and B (Fig. 1). Thus, A is defined as a emission source of ~50 km × 50 km (2500 $km^2$) area, centered in the City of Mendoza, which covers the Great Mendoza territory. B is determined by four emission sources of 16 $km^2$ each, which are 4 km apart one from another, located in the west of the City of Mendoza.

TABLE 2. SUMMARY OF THE EXPERIMENTS CONDUCTED WITH TROPOSPHERIC $SO_4^{2-}$ ARTIFICIAL INJECTION BY MEANS OF WRF/CHEM

| Simulation | Type of $SO_4^{2-}$ | Emission rate, g $s^{-1}$ per $km^2$ | Emission height, km a.s.l. | Emission hours, LT | Sources distribution |
|---|---|---|---|---|---|
| ID1 | SO4I[1] | 30 | 4 | 8–14 | A[3] |
| ID2 | SO4I | 100 | 2 | 8–11 | B[4] |
| | | 50 | 2 | 14–17 | |
| ID1B | SO4I | 30 | 1 | 8 | A |
| ID3 | SO4I | 30 | 4 | 8 | A |
| ID4 | SO4J[2] | 30 | 4 | 8 | A |
| ID5 | SO4I | 1000 | 4 | 8–14 | A |

Note: [1]SO4I – aerosol emissions in Aitken mode, with an average diameter of $D_p$ 0.01 < $D_p$ < 0.1 μm [87]; [2]SO4J – aerosol emissions in Accumulation mode, with 0.1 < $D_p$ < 1 μm; [3]A – 1 emission source of ~50 km · 50 km (2500 $km^2$) area, centered in the City of Mendoza (32° 54' S, 68° 51' W); [4]B – 4 emission sources of 16 $km^2$ area, located in the west of the City of Mendoza.

To analyse the design aspects of a tropospheric $SO_4^{2-}$ artificial injection layer at a regional scale on January 8, 2012, the concept of anomaly on domain D03 was used. On this point, the anomaly of a variable is defined as the difference between the value of a simulation variable with artificial injection of $SO_4^{2-}$ and the corresponding value of the same variable derived from the simulation without injection of aerosols. In addition, the difference between the variables of two experiments with artificial emissions (ID3–ID4) was employed. The concentration of $SO_4^{2-}$ at a specific height, the surface temperature and shortwave solar radiation variables were studied. Furthermore, aspects such as regional atmospheric circulation and radiative balance were analysed using the concept of anomaly.

## 3. RESULTS

Using the ID1–Test_Control and ID2–Test_Control differences, Fig. 8 shows the effects produced by the injection of sulfate aerosols at two different heights on surface temperature and incident radiation shortwave on January 8, 2012 at 12:00 LT. The image shows that the injections of aerosols at 2 and 4 km a.s.l. performed by ID1 (upper panel) and ID2 (lower panel), respectively, increase the concentration of aerosols at such heights (positive anomalies of Fig. 8(a)), thus decreasing solar radiation (negative values of Fig. 8(b)) and surface temperature (negative values of Fig. 8(c)). Additionally, it can be observed that surface temperature anomalies produced by pulsating emissions of ID2 are very similar to those obtained by the continuous emissions derived from ID1. Both experiments produce a mean surface temperature decrease of 0.1 °C at 12:00 LT.

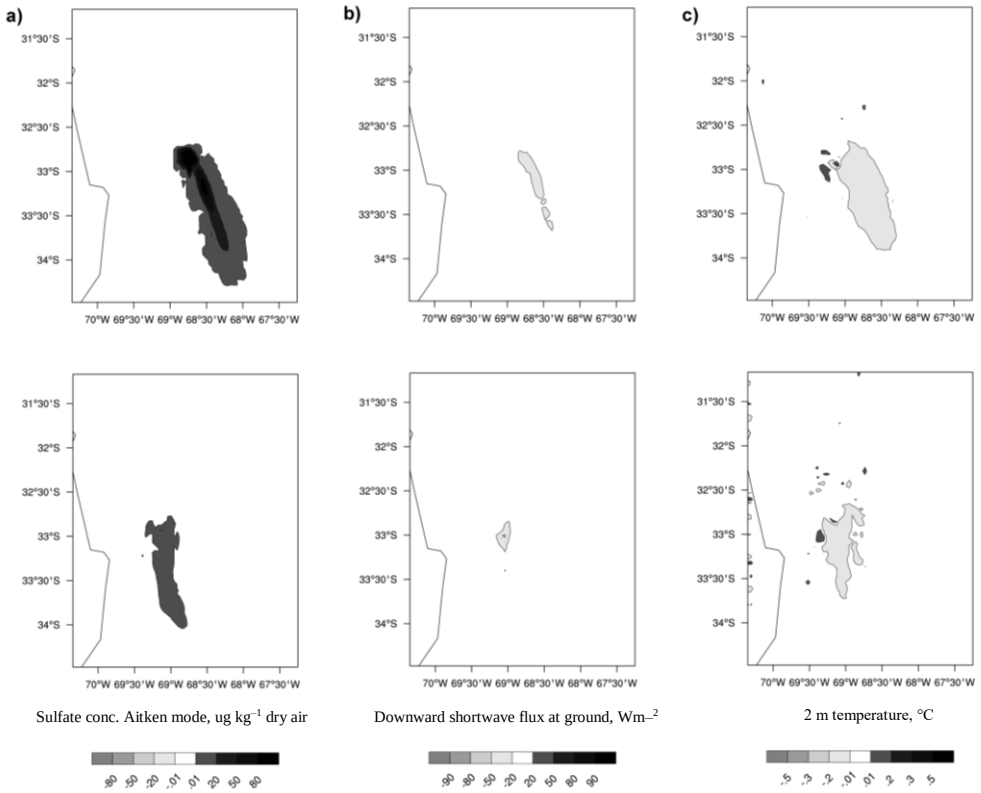


Fig. 8. Anomalies calculated as ID1−Test_Control at 4 km a.s.l. (upper panel) and ID2−Test_Control at 2 km a.s.l. (lower panel) on January 8, 2012 at 12:00 LT for: a) Aitken-mode $SO_4^{2-}$ concentration; b) surface incident shortwave radiation; c) surface temperature.

Based on the same experiments, Fig. 9 shows a vertical cross-section along 32° 54' S latitude of Aitken mode $SO_4^{2-}$ concentration anomaly (see dotted line in Fig. 1(b)). The image indicates that the average sulfate aerosols of ID1 and ID2 experiments remain at 4 and 2 km a.s.l. respectively, for at least 3 hours after the initial injection (performed at 8:00 LT). This situation evidences the ability of the WRF/Chem model to reproduce the stability in the above-mentioned layers. Additionally, using the ID1B−Test_Control difference, Fig. 10 shows the behavior of average sulfate aerosols at 4 km a.s.l in the longitudinal section, taken at latitude of 32° 54' S. The image remarks that the maximum residence time of the aerosol plume at 4 km a.s.l. is approximately 3 hours.

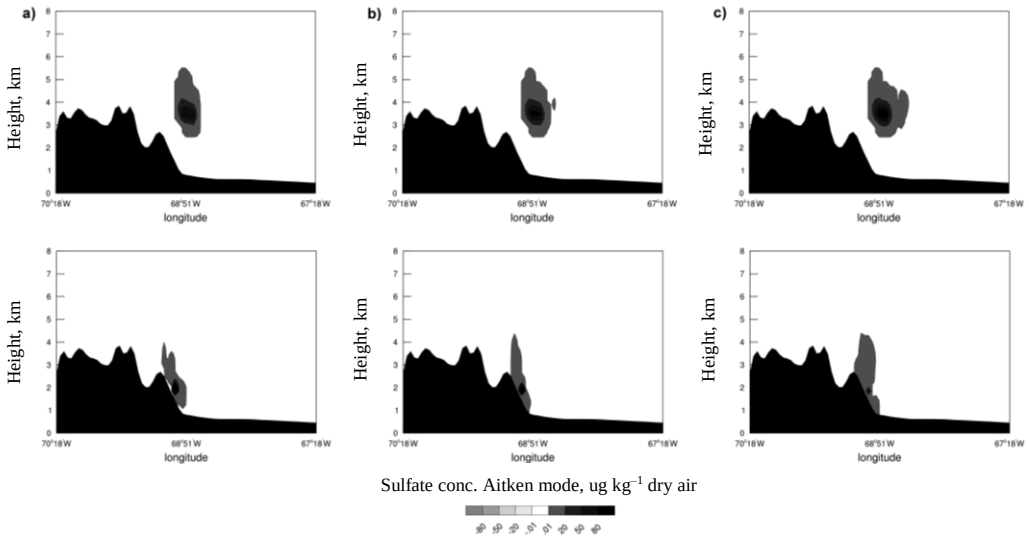


Fig. 9. Cross-sectional profile by longitude and height of Aitken-mode $SO_4^{2-}$ concentration anomaly calculated as ID1−Test_Control at 4 km a.s.l. (upper panel) and ID2−Test_Control at 2 km a.s.l. (lower panel), taken at latitude of 32° 54' S (see dotted line in Fig. 1(b)), for January 8, 2012 at: a) 9:00 LT; b) 10:00 LT; c) 11:00 LT.

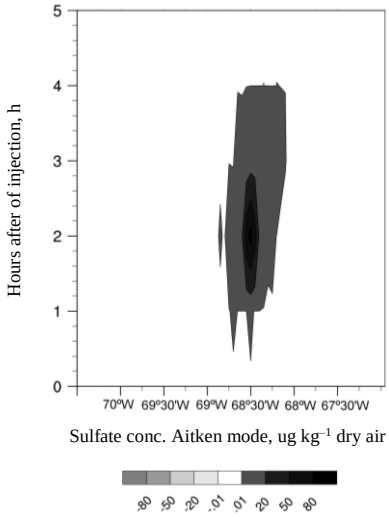


Fig. 10. Time versus longitude section of Aitken-mode $SO_4^{2-}$ concentration anomaly calculated as ID1B−Test_Control at 4 km a.s.l. The analysis is based on concentration averages at 32° 54' S (see dotted line in Fig. 1(b)).

Fig. 11 shows the spatial distribution of aerosols with the Aitken mode (upper panel) and the Accumulation mode (lower panel) at 4 km a.s.l. for 8 January 2012, estimated through ID3−Test_Control. The positive values of the image indicate that the aerosol concentrations of the ID3 with Aitken and Accumulation modes exceed the concentrations of the same size distribution modes of the control test. Therefore, the image suggests that the $SO_4$I emissions of experiment ID1

generate aerosols in the same mode and then they grow to the Accumulation mode. This proves the ability of WRF/Chem to simulate particle growth in the troposphere.

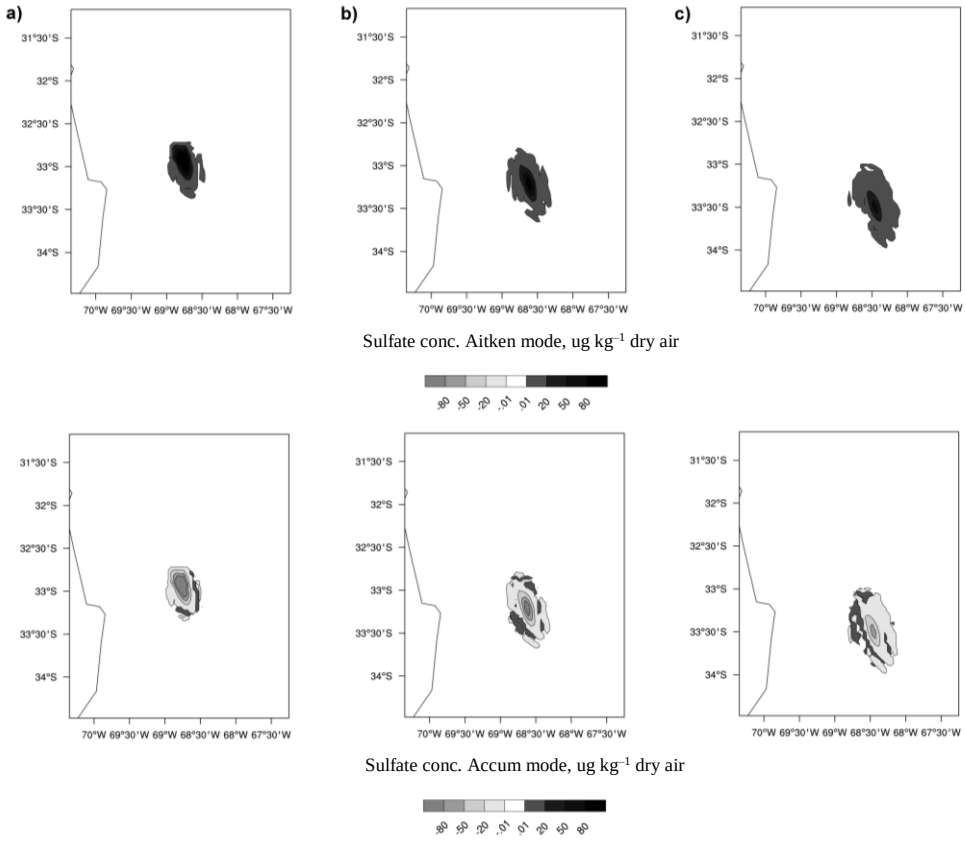


Fig. 11. Aitken-mode (upper panel) and Accumulation-mode (lower panel) $SO_4^{2-}$ concentration anomalies calculated as ID3−Test_Control at 4 km a.s.l. for different hours of 8 January 2012: a) 10:00 LT; b) 11:00 LT; c) 12:00 LT.

The control ability of different configurations of aerosol layers on the target area is analysed below. As of ID3–ID4, Fig. 12 shows the effects of size distribution of sulfate aerosols. In this regard, according to the MADE/SORGAM module, experiment ID3 considers primary emissions with the Aitken mode (SO4I) which generate concentrations with the Aitken and Accumulation modes, while experiment ID4 (with SO4J primary emission) can only produce aerosols in the Accumulation mode. The upper panel of Fig. 12 indicates the plume corresponding to the total (Aitken mode + Accumulation mode) $SO_4^{2-}$ concentration anomaly at 4 km a.s.l., moving in the S-E direction and moving away from the target area (Great Mendoza). The same figure shows that in the center of the plume, experiment ID4 generates higher aerosol concentrations (positive anomalies) than ID3. The lower panel of Fig. 12 shows that negative anomalies (positive) of the surface shortwave radiation are associated to negative (positive) values of aerosol concentration in upper panel of Fig. 12. As well, these latter anomalies indicate that ID4 configuration with $SO_4J$ primary emissions produces a higher (lower) surface incoming solar radiation than the ID3 configuration with $SO_4I$. Thus, a primary emission in Aitken mode would be more suitable than one in the Accumulation mode.

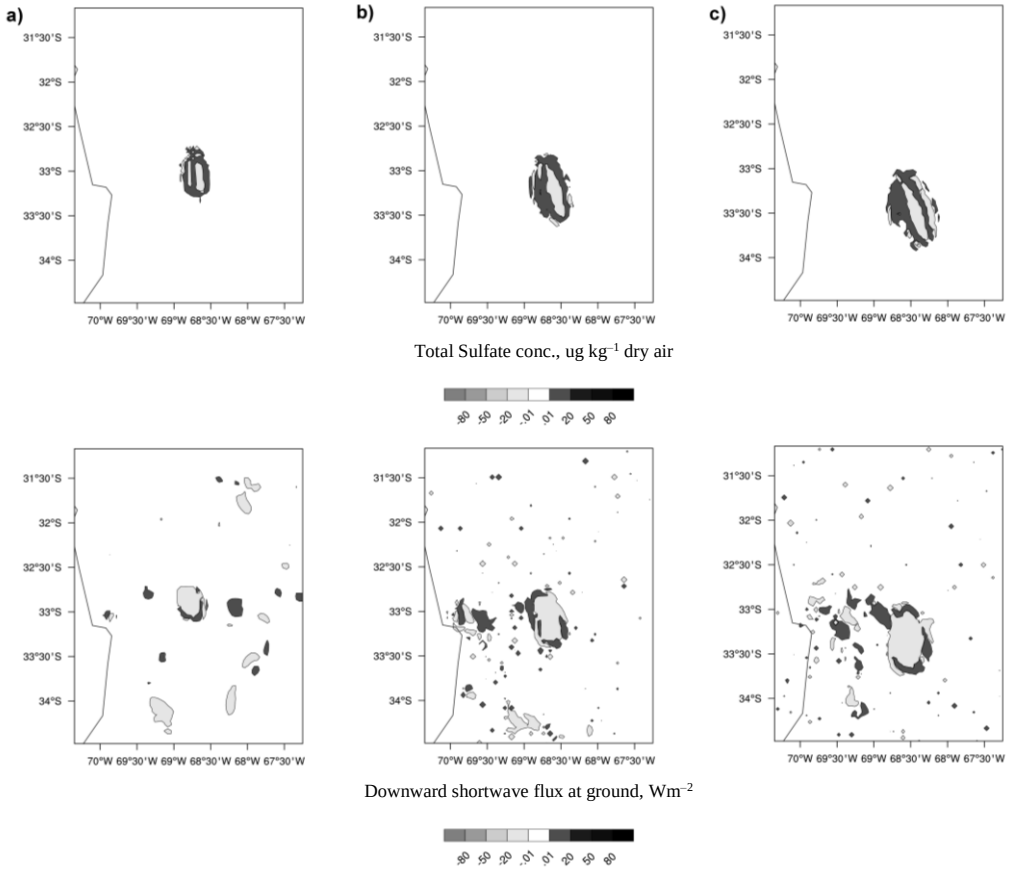


Fig. 12. Anomaly calculated as ID3−ID4 for total (Aitken mode + Accumulation mode) $SO_4^{2-}$ concentration at 4 km a.s.l. (upper panel) and surface incident shortwave radiation on January 8, 2012 at: a) 9:00 LT; b) 10:00 LT; c) 11:00 LT.

Fig. 13 exhibits the effects produced by sulfate aerosols on the radiative balance on January 8, 2012 at 12:00 LT. Table 2 shows that ID5 has the same configuration as ID1, but with a higher rate (1000 g $s^{-1}$ $km^{-2}$ injection). Through the ID5−Test_Control difference, the image shows that ID5 produces a slightly higher aerosol concentration on surface than the aerosol concentration of the control test (< 1 μg $kg^{-1}$ dry air) (Fig. 13(a)), a slight reduction in surface temperature (Fig. 13(b)), a decrease of incoming surface shortwave radiation (Fig. 13(c)) and a loss of non-radiative sensible heat flux (Fig. 13(d)). In comparison to the ID1 rate of 30 g $s^{-1}$ $km^{-2}$ that barely modifies the surface temperature; the ID5 rate of 1000 g $s^{-1}$ $km^{-2}$ could achieve an average decrease of surface temperature of 0.5 °C around Great Mendoza. Such non-radiative flux represents the loss or gain of surface heat by conduction, that is, through heat transfer between the lowest layers of the atmosphere and the surface.

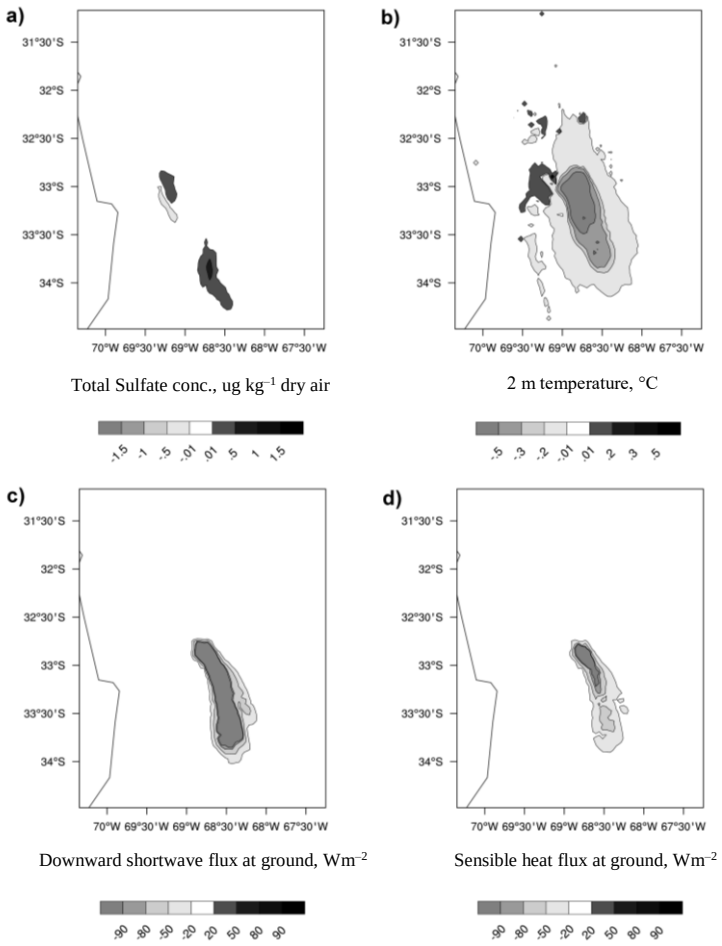


Fig. 13. Anomaly calculated as ID5–Test_Control on January 8, 2012 at 12:00 LT for: a) total (Aitken mode + Accumulation mode) $SO_4^{2-}$ concentration at surface; b) surface temperature; c) surface incident shortwave radiation; d) surface sensitive heat flux.

Considering the ID5–Test_Control difference, Fig. 14 displays the effects of aerosols on the regional atmospheric circulation. Thus, the image shows the differences in horizontal wind speed, geopotential height and vertical wind speed at 2 km a.s.l. on January 8, 2012 at 11:00 LT. The figure reveals that aerosol emissions of experiment ID5 at 4 km a.s.l. produce changes along the atmospheric column. Consequently, in comparison to the control test, the experiment ID5 produces positive horizontal wind speed (dark-grey region of Fig. 14(a)) and negative geopotential height (light-grey region of Fig. 14(b)) anomalies around the City of Mendoza. These latter anomalies are associated to a thin and lower mean temperature layer (colder) related to the negative anomalies of the vertical speed shown in light-grey region of Fig. 14(c).

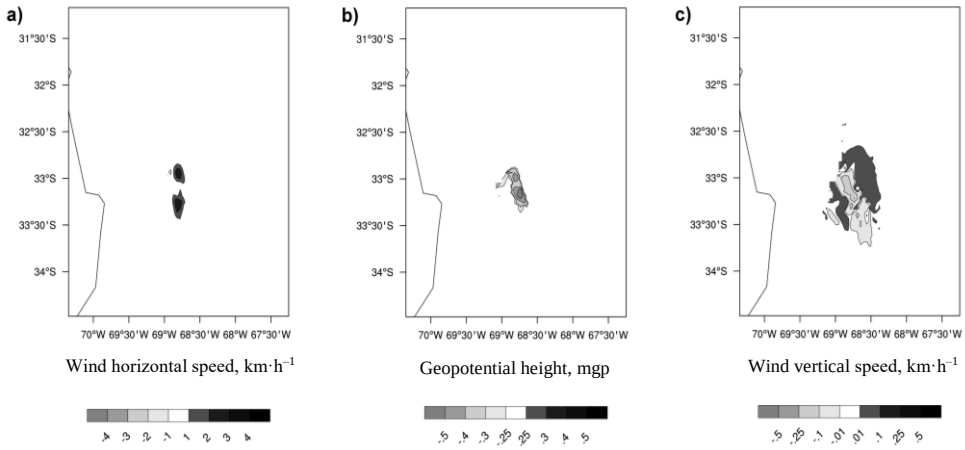


Fig. 14. Anomaly calculated as ID5–Test_Control at 2 km a.s.l. on January 8, 2012 at 11:00 LT for: a) wind horizontal speed; b) geopotential height; c) wind vertical.

## 4. DISCUSSION

A regional operation of tropospheric $SO_4^{2-}$ emissions could be conducted in this research. To reduce the surface temperature by roughly 0.5 °C for 3 consecutive hours approximately, a 1000 g $s^{-1}$ $km^2$ emission rate of $SO_4^{2-}$ is required. This is like injecting an $SO_4^{2-}$ mass of 3.6 ton per hour per $km^2$ into the troposphere with the Aitken mode. To this end, four Cheyenne turboprop aircraft could be used (each with a payload capacity of 1 ton) from the anti-hail program of the Province of Mendoza. In this case, the four Cheyenne turboprop aircraft would emit an additional 4 ton of $CO_2$ per hour per $km^2$, increasing the greenhouse gases (GHG) environmental burden. This environmental cost is estimated by evaluating type of aircraft, flight time, number of take-off and landing cycles, fuel consumption, and fuel emission factor, among others (Table 3). Therefore, to cover 170 $km^2$ of the Great Mendoza territory, 680 ton of $CO_2$ would be emitted. In comparison, 42 500 houses in the same area, using air conditioning systems during 3 hours, for a temperature reduction of 0.5 °C, would emit 150 ton of $CO_2$ (Table 4). This value was obtained considering the mean GHG emissions from electricity supply in Argentina. However, the total variable and fixed direct operating cost inherent to the aeronautical system required to inject the aerosols would be of 3 000 000 USD approximately, in contrast to 21 700 USD derived from the electricity cost of air conditioning use (Table 5). These values are solely estimated for the purposes of an approximate assessment of the environmental and economic cost of both possible solutions and do not imply an exhaustive analysis whatsoever. However, although not fully considered here, the health implications of emitting sulfate aerosols on an urban area will most probably produce huge effects on population health and ecosystems [88]. Eastham et al. [89] have estimated (although with high uncertainties) the impact of stratospheric sulfate geoengineering on mortality from air quality and UV–B exposure, concluding that more than 26 000 premature death per year on a global basis would occur when applying climate engineering. It could be assumed, then, that in the case of tropospheric injections, the death rate would be higher, due to the increase in the air concentration of sulfates by deposition in the study area. However, in the case of heat waves, these emissions would be only eventual, so a conclusion on the subject requires more detailed studies.

TABLE 3. SUMMARY OF THE MAIN CHARACTERISTICS OF THE CHEYENNE AIRCRAFT

| Aircraft information | Cheyenne turboprop |
|---|---|
| Type of fuel used | Aero-Kerosene |
| Kerosene density, kg/l | 0.81 |
| Fuel Consumption at cruise speed, l/h | 265 |
| Fuel Consumption in LTO, l/h | 125 |
| Payload capacity, Tn | 1 |
| Number of aircraft required by $km^2$, to cover 4 Tn | 4 |
| Range per aircraft, h | 1 |
| $CO_2$ emission factor, kg/l | 2.58 |
| $CO_2$ emissions per flight (cruise + LTO), kg/h | 1 006 |

TABLE 4. DATA USED FOR THE ESTIMATION OF CARBON DIOXIDE ($CO_2$) DERIVED FROM THE USE OF AIR CONDITIONING SYSTEMS IN GREAT MENDOZA

| Region | Great Mendoza |
|---|---|
| Area, $km^2$ | 170 |
| Number of inhabitants | 1 500 000 |
| Number of houses per $km^2$ (number of houses per $km^2$) | 250 |
| Houses with air conditioning systems (number of houses in 170 $km^2$) | 42 500 |
| Air conditioning consumption, kWh | 2.4 |
| Supply factor in Argentina, kg $CO_2$/MWh | 490 |

TABLE 5. ECONOMIC COMPARISON BETWEEN ELECTRICAL POWER COST DERIVED FROM THE USE OF AIR CONDITIONING AND THE COST RESULTING FROM THE USE OF CHEYENNE TURBOPROP AIRCRAFT

| Electrical power | | Aircraft | |
|---|---|---|---|
| Cost, USD/MWh | 71 | Total operation cost, USD/h flight | 4 500 |
| Consumption due to the use of air conditioning in 42500 houses, MWh | 102 | Consumption hours, h | 680 |
| Consumption hours, h | 3 | | |
| Consumption in 3 h, MWh | 306 | | |
| Total cost, USD | 21 726 | Total cost, USD | 3 060 000 |

To briefly discuss the tropospheric regional design shown here, it will be compared to a geoengineering application discussed by Heckendorn et al. [50] and English et al. [54]. These works employ a $10^7$ ton injection rate of S per $year^{-1}$ to diminish the global temperature by at least 0.5 °C in a 10 000 000 $km^2$ total surface area (Table 1, [54]). This emission is a very low fraction

compared to 3.6 ton of $SO_4^{2-}$ per hour per km$^2$ proposed in the present study; i.e. approximately 1000 times lower than the emission of sulfur in equivalent terms, considering that 1 ton S is ~3 ton of aerosol particles. This brief analysis suggests that less $SO_4^{2-}$ aerosol injection is required in the lower stratosphere than in the troposphere. Because the injected sulfate aerosols lifetime in the stratosphere is months, compared to a tropospheric lifetime of days [90].

Additionally, the results from the WRF/Chem model used in Bernstein et al. [56] and our research suggests that the inclusion of sulfate layer in atmosphere reduces surface temperature at urban and regional scales. In this respect, for example, the metropolitan-scale 30 μg m$^{-2}$ s$^{-1}$ at 12 km altitude considered by Bernstein et al. produced a mean surface temperature decrease of 2 °C at the time of solar noon (Fig. 14 by [56]). This reduction is roughly 20 times larger than the surface air temperature reductions over Great Mendoza, considering the same emission rate at 4 km a.s.l. (see result of ID1 design by Fig. 8). While the injection Bernstein et al corresponds to 360 ton of sulfate aerosols integrated over 1 700 km$^2$ and 2 hr; our injection was of 1 600 ton of aerosols integrated over 2 500 km$^2$ and 6 hours injections interval (see ID1 experiment in Table 2).

The choice of the parameters of engineering injection in both studies mainly depends on the specific meteorological conditions. These simulations were carried out around at 30 degrees of latitude to the equator in both hemispheres, which are influenced to midlatitude frontal systems. Thereby, Bernstein et al. chose the 12 km a.s.l. injection height based solely on local considerations of minimal flow (roughly 14 to 50 km h$^{-1}$) for a specific city at a time just before the start of the injections. In our case, the 2 and 4 km a.s.l. injection heights were determined based on wind speed, direction and persistence, and atmospheric thermal stability on their respective layers. A stratospheric injection, near the tropopause, such as that made by Bernstein et al., is not possible due to fast westerly wind speed over the Province of Mendoza. Moreover, both researches insert aerosols during the morning hours which allow them to act at the hours of maximum temperatures. In this respect, Bernstein et al. injected aerosols between 06:00 and 08:00 LT and we inserted aerosols at 8:00 LT during from 1 to 6 h.

This previous analysis shows how as injection altitudes move from stratosphere and near tropopause to troposphere, better spatial control at small scales may be possible, but at higher injections rate.

The studies are influenced by the aerosol module selected to simulate sulfate size-distribution. In this aspect, Bernstein et al. used the MOSAIC sectional approach where the size distribution is discretized into four sections and sulfate properties are assumed to be constant over particle size sections [91]. Instead, we adopted the MADE/SORGAM modal treatment where the size distribution is approximated by Aitken and Accumulation modes and standard deviation is assumed to be constant in each mode. The latter approach reduces MADE/SORGAM complexity, consuming less computational resources than MOSAIC. However, it may also induce errors in the aerosol number and mass concentrations [92], [93]. The amount of recent research comparing MADE/SORGAM and MOSAIC modules suggests the lack of consensus to use a specific aerosol model (e.g., [93], [94]). Thereby, a comprehensive approach that evaluates all model components is needed to assess the true performance of specific aerosol process modules over Province of Mendoza.

In summary, two types of climate engineering approaches are currently being considered in the literature: one on a global scale aiming at long term temperature reduction and a second one on short-term local/regional scale application to offset the impact of heat waves. Although both try to take advantages of sulfate aerosol properties, the technological designs are very different. In the tropospheric case, design trade off requires the search of low wind and stable layers, which determine the size and frequency of the injection. In the stratospheric case, less $SO_4^{2-}$ aerosol emissions are required because the aerosols are injected in a stable layer reaching higher lifetime [55].

## 5. CONCLUSIONS

The primary objective of this research was to examine whether aerosol emissions, considered by geoengineering on a global scale [95], might be applied to mitigate meteorological phenomena with extremely high daily temperatures on a regional scale.

The specific objectives of this work were:

1) to model the behaviour of $SO_4^{2-}$ aerosols in the troposphere and their influence on temperature and surface incident solar radiation, at the regional scale, using an appropriate online coupled mesoscale meteorology and chemistry model;

2) to determine the main geoengineering design parameters using tropospheric $SO_4^{2-}$ aerosols in order to artificially reduce temperature and incoming radiation on surface during short-time events of extremely high daily temperatures, and

3) to evaluate a preliminary technical proposal for the injection of regionally engineered tropospheric $SO_4^{2-}$ aerosols.

In order to accomplish the abovementioned objectives, we used the WRF/Chem [57], [58] to model and evaluate the behaviour of tropospheric $SO_4^{2-}$ at the regional scale over the Province of Mendoza (Argentina) on a clear sky day during a heat wave event which occurred in January 2012. In addition, using WRF/Chem, we evaluated the potential reductions in temperature and incident shortwave incoming radiation on surface around the metropolitan area of Great Mendoza based on an artificially designed aerosol layer and on observed meteorological parameters.

In the first place, this research showed the ability of WRF/Chem to model the behaviour of anthropogenic tropospheric $SO_4^{2-}$ aerosols on a regional scale, their influence on the temperature and on the incident solar radiation at surface, for diverse emission modes and rates.

In this regard, the numerical modelling with WRF/Chem suggests that the inclusion of $SO_4^{2-}$ aerosols in the troposphere, results in a surface temperature reduction. In addition, the aerosol, with appropriate physical and radiative properties, can modify the energy balance on the surface, by means of the alteration of the incoming shortwave radiation components and the non-radiative sensible heat flux, and atmospheric circulation patterns. The maximum negative anomalies of temperature with a mean reduction of 0.5 °C, in a $4 \cdot 4$ km$^2$ grid, were registered at an emission rate of 1000 g s$^{-1}$ km$^{-2}$.

This research further shows that WRF/Chem is capable of suitably reproducing meteorological conditions and atmospheric stability related to the period of study.

Second, the following conclusions on the tropospheric $SO_4^{2-}$ aerosol layer design were derived from the regional modelling:

- The aerosol must have a size distribution of Aitken mode (Dp < 0.1 μm);
- The emission height was located at 4 km a.s.l. (600 hPa) and the minimum height of injection was set at 2 km a.s.l. (850 hPa) above the upper limit of the planetary boundary layer;
- The operating cycle of $SO_4^{2-}$ emission is high (1 hour of emission for every 3 hours without emission);
- The emission rate that produces significant effects on the surface temperature is >1000 g s$^{-1}$ per km$^2$. It is recommended that the higher the emission rate, the more it should be placed above 2 km a.s.l.

Third, this research evaluated a preliminary method of tropospheric $SO_4^{2-}$ aerosol injection based on the current anti-hail program of the Province of Mendoza. In this regard, it is estimated that to inject 3.6 ton of $SO_4^{2-}$ per km$^2$ per hour in the Aitken mode, four Cheyenne turboprop aircraft may be used. However, the use of those airplanes would be associated to a higher environmental cost of

$CO_2$ emissions than those originated from the use of air conditioning systems in the Province of Mendoza.

Finally, it is concluded that, based on the physical and radiative properties of tropospheric $SO_4^{2-}$, and under meteorological conditions associated to heat wave events, extremely high daily temperatures on a regional scale are likely to be reduced by means of the artificial injection of the abovementioned aerosols. However, although the results of this research are not conclusive, the high rate of injection and the large amount of mass required for its practical implementation in the Province of Mendoza by means of the technology currently used by the anti-hail program, makes it inefficient and energetically costly. The method further showed that the action of the aerosols cannot be limited to a restricted area and, as a result, effects outside the limits of the area of interest are likely to be observed. In concordance with previous studies, our results indicate that a large tropospheric emission of sulfate aerosols close to the target region might indeed have substantial impacts on precipitation, population health and ecosystems [55], [56], [88].

The case study here was over the Province of Mendoza, which has an outstanding environmental regulation and policy, and therefore, it is expected that the regional-scale sulfate aerosol application will receive a very careful review and oversight. This study, performed on a specific day, might serve as a guide for other cases of tropospheric $SO_4^{2-}$ aerosol injection during heat wave events.

## ACKNOWLEDGEMENT

Authors acknowledge the National Centers for Environmental Prediction (NCEP) for the GFS analysis dataset with documentation available on [73]. Authors also gratefully acknowledge Earth System Research Laboratory of the National Oceanic and Atmospheric Administration [72], REanalysis of the TROpospheric chemical composition (RETRO: [82]) and Emission Database for Global Atmospheric Research (EDGAR: [83]) for processing and distributing data used in this article. The authors gratefully acknowledge the assistance of the editor-in-chief of Environmental and Climate Technologies, PhD. Zane Indzere, in editing the manuscript and the anonymous reviewer for his/her detailed and helpful comments to the manuscript. This work was supported by Consejo Nacional de Investigaciones Científicas y Técnicas (CONICET), Universidad Tecnológica Nacional (UTN) and Pontificia Universidad Católica Argentina (UCA).

## ADDITIONAL INFORMATION

We want to highlight that:

1) the paper is original and has not been published or sent to another Journal for publication;
2) the author and co-authors declare that they have no competing interests, financial or otherwise;
3) authors declare acceptance of the copyright conditions specified therein with the submission of this paper.

## REFERENCES

[1] Haywood J., Boucher O. Estimates of the direct and indirect radiative forcing due to tropospheric aerosols: A review. *Reviews of Geophysics* 2000:38(4):513–543. doi:10.1029/1999RG000078

[2] Deshler T. A review of global stratospheric aerosol: Measurements, importance, life cycle, and local stratospheric aerosol. *Atmospheric Research* 2008:90(2–4):223–232. doi:10.1016/j.atmosres.2008.03.016

[3] Gu Y., Liou K. N., Chen W., Liao H. Direct climate effect of black carbon in China and its impact on dust storms. *Journal of Geophysical Research* 2010:115:D00K14. doi:10.1029/2009JD013427

[4] Papadimas C. D., et al. The direct effect of aerosols on solar radiation over the broader Mediterranean basin. *Atmospheric Chemistry and Physics* 2012:12(15):7165–7185. doi:10.5194/acp−12−7165−2012

[5] Hansen J., Sato M., Ruedy R. Radiative forcing and climate response. *Journal of Geophysical Research*. 1997:102(D6):6831–6864. doi:10.1029/96JD03436

[6] Schell B., Ackermann I. J., Hass H., Binkowski F. S., Ebel A. Modeling the formation of secondary organic aerosol within a comprehensive air quality model system. *Journal of Geophysical Research: Atmospheres* 2001:106(D22):28275–28293. doi:10.1029/2001JD000384

[7] Liou K.-N., Ou S.-C. The role of cloud microphysical processes in climate: An assessment from a one-dimensional perspective. *Journal of Geophysical Research: Atmospheres* 1989:94(D6):8599–8607. doi:10.1029/JD094iD06p08599

[8] Rosenfeld D. Suppression of Rain and Snow by Urban and Industrial Air Pollution. *Science* 2000:287(5459):1793–1796. doi:10.1126/science.287.5459.1793

[9] Borys R. D., Lowenthal D. H., Mitchell D. L. The relationships among cloud microphysics, chemistry, and precipitation rate in cold mountain clouds. *Atmospheric Environment* 2000:34(16):2593–2602. doi:10.1016/S1352−2310(99)00492−6

[10] Shepherd J. M., Burian S. J. Detection of Urban-Induced Rainfall Anomalies in a Major Coastal City. *Earth Interactions* 2003:7(4):1–17. doi:10.1175/1087−3562(2003)007%3c0001:DOUIRA%3e2.0.CO;2

[11] Cullis C. F., Hirschler M. M. Atmospheric sulphur: Natural and man−made sources. *Atmospheric Environment* 1980:14(11):1263–1278. doi:10.1016/0004−6981(80)90228−0

[12] Penner J. E., Lister D., Griggs D. J., McFarland M., Dokken D. J. Aviation and the global atmosphere: a special report of the Intergovernmental Panel on Climate Change. Cambridge: Cambridge University Press, 1999.

[13] Günther A., et al. MIPAS observations of volcanic sulfate aerosol and sulfur dioxide in the stratosphere. *Atmospheric Chemistry and Physics* 2018:18(2):1217–1239. doi:10.5194/acp−2017−538

[14] Pitari G., et al. Sulfate Aerosols from Non-Explosive Volcanoes: Chemical-Radiative Effects in the Troposphere and Lower Stratosphere. *Atmosphere* 2016:7(7):85. https://doi.org/10.3390/atmos7070085

[15] Stenchikov G. L., et al. Radiative forcing from the 1991 Mount Pinatubo volcanic eruption. *Journal of Geophysical Research: Atmospheres* 1998:103(D12):13837–13857. doi:10.1029/98JD00693

[16] Charlson R. J., et al. Climate forcing by anthropogenic aerosols. *Science* 1992:255(5043):423–30. doi:10.1126/science.255.5043.423

[17] Kiehl J. T., Briegleb B. P. The relative roles of sulfate aerosols and greenhouse gases in climate forcing. *Science* 1993:260(5106):311–4. doi:10.1126/science.260.5106.311

[18] Jiandong L., Jiangyu M., Wei-Chyung W. Anthropogenic Eastern Asian radiative forcing due to sulfate and black carbon aerosols and their time evolution estimated by an AGCM. *Chinese Journal of Geophysics* 2015:58(4):1103–1120.

[19] McCormick M. P., Thomason L. W., Trepte C. R. Atmospheric effects of the Mt Pinatubo eruption. *Nature* 1995:373(6513):399–404. doi:10.1038/373399a0

[20] Michelangeli D. V., Allen M., Yung Y. L. El Chichon volcanic aerosols: Impact of radiative, thermal, and chemical perturbations. *Journal of Geophysical Research* 1989:94(D15):18429. doi:10.1029/JD094iD15p18429

[21] Boucher O., et al. Clouds and Aerosols. In: Climate Change 2013: The Physical Science Basis. Contribution of Working Group I to the Fifth Assessment Report of the Intergovernmental Panel on Climate Change. Cambridge: Cambridge University Press, 2013:571–657.

[22] Jones A., Roberts L., Wood J., Johnson C. E. Indirect sulphate aerosol forcing in a climate model with an interactive sulphur cycle. *Journal of Geophysical Research: Atmospheres* 2001:106(D17):293–313. doi:10.1029/2000JD000089

[23] Trenberth K., Dai A. Effects of Mount Pinatubo volcanic eruption on the hydrological cycle as an analog of geoengineering. *Geophysical Research Letters* 2007:34(15). doi:10.1029/2007GL030524

[24] Friberg J., et al. Influence of volcanic eruptions on midlatitude upper tropospheric aerosol and consequences for cirrus clouds. *Earth and Space Science* 2015:2(7):285–300. doi:10.1002/2015EA000110

[25] Ramanathan V., Carmichael G. Global and regional climate changes due to black carbon. *Nature Geoscience* 2008:1(4):221–227. doi:10.1038/ngeo156

[26] Forster P., et al. Climate Change 2007: The Physical Science Basis : Contribution of Working Group I to the Fourth Assessment Report of the Intergovernmental Panel on Climate Change. Cambridge: Cambridge University Press, 2007.

[27] Shindell D., Faluvegi G. Climate response to regional radiative forcing during the twentieth century. *Nature Geoscience* 2009:2(4):294–300. doi:10.1038/ngeo473

[28] Giorgi F., Bi X., Qian Y. Indirect vs. Direct Effects of Anthropogenic Sulfate on the Climate of East Asia as Simulated with a Regional Coupled Climate-Chemistry/Aerosol Model. *Climatic Change* 2003:58(3):345–376. doi:10.1023/A:1023946010350

[29] Giorgi F., Bi X., Qian Y. Direct radiative forcing and regional climatic effects of anthropogenic aerosols over East Asia: A regional coupled climate-chemistry/aerosol model study. *Journal of Geophysical Research: Atmospheres* 2002:107(D20):AAC–7. doi:10.1029/2001JD001066

[30] Qian Y., Giorgi F. Regional climatic effects of anthropogenic aerosols? The case of southwestern China. *Geophysical Research Letters* 2000:27(21):3521–3524. doi:10.1029/2000GL011942

[31] Wu J., Luo Y., Wang W. The comparison of different simulation methods for the climate responses of the radiative forcing of anthropogenic sulfate aerosol over east Asia. *Journal of Yunnan University* 2005:27(4):323–331.

[32] Ekman A. M. L., Rodhe H. Regional temperature response due to indirect sulfate aerosol forcing: impact of model resolution. *Climate Dynamics* 2003:21(1):1–10. doi:10.1007/s00382−003−0311−y

[33] Foote G. B., Knight C. A. Results of a Randomized Hail Suppression Experiment in Northeast Colorado. Part I: Design and Conduct of the Experiment. *Journal of Applied Meteorology* 1979:18(12):1526–1537. doi:10.1175/1520−0450(1979)018%3c1526:ROARHS%3e2.0.CO;2

[34] García-Ortega E., López L., Sánchez J. L. Diagnosis and sensitivity study of two severe storm events in the Southeastern Andes. *Atmospheric research* 2009:93(1–3):161–178. doi:10.1016/j.atmosres.2008.10.030

[35] Silverman B. A. A Critical Assessment of Glaciogenic Seeding of Convective Clouds for Rainfall Enhancement. *Bulletin of the American Meteorological Society* 2001:82(5):903–923. doi:10.1175/1520−0477(2001)082%3c0903:ACAOGS%3e2.3.CO;2

[36] Miao Q., Geerts B. Airborne measurements of the impact of ground-based glaciogenic cloud seeding on orographic precipitation. *Advances in Atmospheric Sciences* 2013:30(4):1025–1038. doi:10.1007/s00376-012-2128-2

[37] Rasch P., et al. An overview of geoengineering of climate using stratospheric sulphate aerosols. *Philosophical transactions. Series A, Mathematical, physical, and engineering sciences* 2008:366(1882):4007–4037. doi:10.1098/rsta.2008.0131

[38] Crutzen P. J. Albedo enhancement by stratospheric sulfur injections: A contribution to resolve a policy dilemma? *Climatic Change* 2006:77(3–4):211–220. doi:10.1007/s10584–006–9101–y

[39] Groisman P. Possible regional climate consequences of the Pinatubo eruption: an empirical approach. *Geophysical Research Letters* 1992:19(15):1603–1606. doi:10.1029/92GL01474

[40] Kirchner I., Stenchikov G. L., Graf H.-F., Robock A., Antuña J. C. Climate model simulation of winter warming and summer cooling following the 1991 Mount Pinatubo volcanic eruption. *Journal of Geophysical Research* 1999:104(D16):19039–19055. doi:10.1029/1999JD90021

[41] Govindasamy B., Caldeira K. Geoengineering Earth's radiation balance to mitigate $CO^{2-}$ induced climate change. *Geophysical Research Letters* 2000:27(14):2141–2144. doi:10.1029/1999GL006086

[42] Keith D. W. Photophoretic levitation of engineered aerosols for geoengineering. *Proceedings of the National Academy of Sciences* 2010:107(38):16428–16431. doi:10.1073/pnas.1009519107

[43] Aquila V., Garfinkel C. I., Newman P. A., Oman L. D., Waugh D. W. Modifications of the quasi-biennial oscillation by a geoengineering perturbation of the stratospheric aerosol layer. *Geophysical Research Letters* 2014:41(5):1738–1744. doi:10.1002/2013GL05881

[44] Pitari G., et al. Stratospheric ozone response to sulfate geoengineering: Results from the Geoengineering Model Intercomparison Project (GeoMIP). *Journal of Geophysical Research: Atmospheres* 2014:119(5):2629–2653. doi:10.1002/2013JD020566

[45] Kravitz B., Robock A., Boucher O., Schmidt H., Taylor K. E., Stenchikov G., Schulz M. The geoengineering model intercomparison project (GeoMIP). *Atmospheric Science Letters* 2011:12(2):162–167. doi:10.1002/asl.316

[46] MacMartin D. G., et al. The climate response to stratospheric aerosol geoengineering can be tailored using multiple injection locations. *Journal of Geophysical Research: Atmospheres* 2017:122(23):12–574. doi:10.1002/2017JD02687

[47] Tilmes S., et al. Sensitivity of aerosol distribution and climate response to stratospheric $SO_2$ injection locations. *Journal of Geophysical Research: Atmospheres* 2017:122(23):12591–12615. doi:10.1002/2017JD026888

[48] Laakso A., Korhonen H., Romakkaniemi S., Kokkola H. Radiative and climate effects of stratospheric sulfur geoengineering using seasonally varying injection areas. *Atmospheric Chemistry and Physics* 2017:17(11):6957. doi:0.5194/acp−2017−107

[49] Rasch P., Crutzen J., Coleman B. Exploring the geoengineering of climate using stratospheric sulfate aerosols: The role of particle size. *Geophysical Research Letters* 2008:35(2). doi:10.1029/2007GL032179

[50] Heckendorn P., et al. The impact of geoengineering aerosols on stratospheric temperature and ozone. *Environmental Research Letters* 2009:4(4):045108. doi:10.1088/1748−9326/4/4/045108

[51] Niemeier U., Timmreck C., Graf H.-F., Kinne S., Rast S., Self S. Initial fate of fine ash and sulfur from large volcanic eruptions. *Atmospheric Chemistry and Physics* 2009:9(22):9043–9057. doi:10.5194/acp−9−9043−2009

[52] Pierce J. R., et al. Efficient formation of stratospheric aerosol for climate engineering by emission of condensible vapor from aircraft. *Geophysical Research Letters* 2010:37(18). doi:10.1029/2010GL043975

[53] Vattioni S., Weisenstein D., Keith D., Feinberg A., Peter T., Stenke A. Exploring accumulation-mode-$H_2SO_4$ versus $SO_2$ stratospheric sulfate geoengineering in a sectional aerosol-chemistry-climate model. *Atmospheric Chemistry and Physics Discussions* 2018:1–30. doi:10.5194/acp−2018−1070

[54] English J. M., Toon O. B., Mills M. J. Microphysical simulations of sulfur burdens from stratospheric sulfur geoengineering. *Atmospheric Chemistry and Physics* 2012:12(10):4775–4793. doi:10.5194/acp−12−4775−2012

[55] Visioni D., Pitari G., Tuccella P., Curci G. Sulfur deposition changes under sulfate geoengineering conditions: Quasi-biennial oscillation effects on the transport and lifetime of stratospheric aerosols. *Atmospheric Chemistry and Physics* 2018:18(4):2787–2808. doi:10.5194/acp−18−2787−2018

[56] Bernstein D. N., Neelin J. D., Li Q. B., Chen D. Could aerosol emissions be used for regional heat wave mitigation? *Atmospheric Chemistry and Physics* 2013:13(13):6373–6390.

[57] Grell G. A., et al. Fully coupled "online" chemistry within the WRF model. *Atmospheric Environment* 2005:39(37):6957–6975. doi:10.1016/j.atmosenv.2005.04.027

[58] Skamarock W. C., et al. A Description of the Advanced Research WRF Version 3. NCAR Technical Note NCAR/TN–475+STR. Boulder: NSCAR, 2008. doi:10.5065/D68S4MVH
[59] Sánchez J. L., López L., García-Ortega E., Gil B. Nowcasting of kinetic energy of hail precipitation using radar. *Atmospheric Research* 2013:123:48–60. doi:10.1016/j.atmosres.2012.07.021
[60] Zanobetti A., O'Neill M. S., Gronlund C. J., Schwartz J. D. Susceptibility to mortality in weather extremes: effect modification by personal and small-area characteristics. *Epidemiology* 2013:24(6):809–19. doi:10.1097/01.ede.0000434432.06765.91
[61] Ciais P., et al. Europe-wide reduction in primary productivity caused by the heat and drought in 2003. *Nature* 2005:437(7058):529–33. doi:10.1038/nature03972
[62] Toomey M., Roberts D. A., Still C., Goulden M. L., McFadden J. P. Remotely sensed heat anomalies linked with Amazonian forest biomass declines. *Geophysical Research Letters* 2011:38(19). doi:10.1029/2011GL049041
[63] Smoyer-Tomic K. E., Kuhn R., Hudson A. Heat Wave Hazards: An Overview of Heat Wave Impacts in Canada. *Natural Hazards* 2003:28(2–3):465–486. doi:10.1023/A:1022946528157
[64] Roper R. E. Book Review of Heat Wave: A Social Autopsy of Disaster in Chicago by E. Klinenberg. *The American Journal of Sociology* 2003:108(5):1114–1115.
[65] Jolly W. M., Dobbertin M., Zimmermann N. E., Reichstein M. Divergent vegetation growth responses to the 2003 heat wave in the Swiss Alps. *Geophysical Research Letters* 2005:32(18). doi:10.1029/2005GL023252
[66] Theoharatos G., Pantavou K., Mavrakis A., Spanou A., Katavoutas G., Efstathiou P., Mpekas P., Asimakopoulos D. Heat waves observed in 2007 in Athens, Greece: synoptic conditions, bioclimatological assessment, air quality levels and health effects. *Environmental research* 2010:110(2):152–61. doi:10.1016/j.envres.2009.12.002
[67] Rusticucci M., Kyselý J., Almeira G., Lhotka O. Long-term variability of heat waves in Argentina and recurrence probability of the severe 2008 heat wave in Buenos Aires. *Theoretical and Applied Climatology* 2015:124(3–4):679–689.
[68] Cerne S. B., Vera C. S., Liebmann B. The Nature of a Heat Wave in Eastern Argentina Occurring during SALLJEX. *Monthly Weather Review* 2007:135(3):1165–1174. doi:10.1175/MWR3306.1
[69] Norte F. A., Seluchi M. E., Gomes J. L., Simonelli S. C. Analysis of an extreme heat wave over the subtropical region of South America. *Revista Brasileira de Meteorologia* 2007:22(3):373–386. doi.org/10.1590/S0102-77862007000300010
[70] Ente Provincial Regulador Eléctrico. Evolución de la demanda de electricidad de Mendoza ante la ola de calor-Última semana 2011 y comienzos 2012, 2011.
Available: http://epremendoza.gov.ar/_a_adjuntos/Evol_Demanda_Ola_Calor_2011_2012.pdf
[71] Flores G.E., Gómez R.S. Taxonomía y biogeografía de cuatro especies de Psectrascelis (Coleoptera: Tenebrionidae) de la Precordillera y Cordillera de los Andes en Mendoza, Argentina. *Revista de la Sociedad Entomológica Argentina*. 2005:64(3):93–106.
[72] U.S. Department of Commerce. National Oceanic and Atmospheric Administration, Earth System Research Laboratory, Physical Sciences Division. Daily Climate Composites. Available: https://www.esrl.noaa.gov/psd/data/composites/day/
[73] National Center for Atmospheric Research. Historical Unidata Internet Data Distribution Gridded Model Data, 2003. doi:10.5065/549X-KE89
[74] Almanza V. H., Molina L. T., Li G., Fast J., Sosa G. Impact of external industrial sources on the regional and local $SO_2$ and $O_3$ levels of the Mexico megacity. *Atmospheric Chemistry and Physics* 2014:14(16):8483–8499. doi:10.5194/acp−14−8483−2014
[75] Chapman E. G., et al. Coupling aerosol-cloud-radiative processes in the WRF-Chem model: Investigating the radiative impact of elevated point sources. *Atmospheric Chemistry and Physics* 2009:9(3):945–964. doi:10.5194/acp−9−945−2009
[76] Misenis C., Zhang Y. An examination of sensitivity of WRF/Chem predictions to physical parameterizations, horizontal grid spacing, and nesting options. *Atmospheric Research* 2010:97(3):315–334. doi:10.1016/j.atmosres.2010.04.005
[77] Mulena G. C., Allende D. G., Puliafito S. E., Lakkis S. G., Cremades P. G., Ulke A. G. Examining the influence of meteorological simulations forced by different initial and boundary conditions in volcanic ash dispersion modelling. *Atmospheric Research* 2016:176–177:29–42. doi:10.1016/j.atmosres.2016.02.009
[78] Carvalho D., Rocha A., Gómez-Gesteira M. Ocean surface wind simulation forced by different reanalyses: Comparison with observed data along the Iberian Peninsula coast. *Ocean Modelling* 2012:56:31–42. doi:10.1016/j.ocemod.2012.08.002
[79] Borge R., Alexandrov V., Josedelvas J., Lumbreras J., Rodriguez E. A comprehensive sensitivity analysis of the WRF model for air quality applications over the Iberian Peninsula. *Atmospheric Environment* 2008:42(37):8560–8574. doi:10.1016/j.atmosenv.2008.08.032
[80] Stockwell W. R., Middleton P., Chang J. S., Tang X. The second generation regional acid deposition model chemical mechanism for regional air quality modeling. *Journal of Geophysical Research* 1990:95(D10):16343. doi:10.1029/JD095iD10p16343

[81] Ackermann I. J., Hass H., Memmesheimer M., Ebel A., Binkowski F. S., Shankar U. Modal aerosol dynamics model for Europe: development and first applications. *Atmospheric Environment* 1998:32(17):2981–2999. doi.org/10.1016/S1352-2310(98)00006-5

[82] Max Planck Institute for Meteorology. REanalysis of the TROpospheric chemical composition over the past 40 years (RETRO). A long-term global modeling study of tropospheric chemistry funded under the 5th EU framework programme. Report no. 48/2007 of the Max Planck Institute for Meteorology, 2007.

[83] Olivier J. G. J., et al. Applications of Emission Database for Global Atmospheric Research (EDGAR). Including a description of EDGAR 3.2. Reference database with trend data for 1970−1995. *INIS* 2002:33(45).

[84] National Emissions Inventory (NEI). United States Environmental Protection Agency (U.S. EPA). Available: https://www.epa.gov/air-emissions-inventories/national-emissions-inventory-nei

[85] Ginoux P., Chin M., Tegen I., Prospero J. M., Holben B., Dubovik O., Lin S.-J. Sources and distributions of dust aerosols simulated with the GOCART model. *Journal of Geophysical Research* 2001:106(D17):20255. doi:10.1029/2000JD000053

[86] Guenther A., Karl T., Harley P., Wiedinmyer C., Palmer P. I., Geron C. Estimates of global terrestrial isoprene emissions using MEGAN (Model of Emissions of Gases and Aerosols from Nature). *Atmospheric Chemistry and Physics* 2006:6(11):3181–3210. doi.org/10.5194/acp-6-3181-2006

[87] Seinfeld J. H., Pandis S. N. Atmospheric Chemistry and Physics: From Air Pollution to Climate Change, 2nd Edition. NY: Wiley, 2006.

[88] Kravitz B., Robock A., Oman L., Stenchikov G., Marquardt A. B. Sulfuric acid deposition from stratospheric geoengineering with sulfate aerosols. *Journal of Geophysical Research* 2009:114(D14):D14109. doi:10.1029/2009JD011918

[89] Eastham S. D., Weisenstein D. K., Keith D. W., Barrett S. R. H. Quantifying the impact of sulfate geoengineering on mortality from air quality and UV-B exposure. *Atmospheric Environment* 2018:187:424–434. doi:10.1016/J.ATMOSENV.2018.05.047

[90] Visioni D., Pitari G., Aquila V. Sulfate geoengineering: a review of the factors controlling the needed injection of sulfur dioxide. *Atmospheric Chemistry and Physics* 2017:17(6):3879–3889. doi:10.5194/acp-17-3879-2017

[91] Zaveri R. A., Easter R. C., Fast J. D., Peters L. K. Model for Simulating Aerosol Interactions and Chemistry (MOSAIC). *Journal of Geophysical Research* 2008:113(D13):D13204. doi:10.1029/2007JD008782

[92] Zhang Y., Seigneur C., Seinfeld J. H., Jacobson M. Z., Binkowski F. S. Simulation of Aerosol Dynamics: A Comparative Review of Algorithms Used in Air Quality Models. *Aerosol Science and Technology* 1999:31(6):487–514. doi:10.1080/027868299304039

[93] Zhang Y., He J., Zhu S., Gantt B. Sensitivity of simulated chemical concentrations and aerosol-meteorology interactions to aerosol treatments and biogenic organic emissions in WRF/Chem. *Journal of Geophysical Research: Atmospheres* 2016:121(10):6014–6048. doi:10.1002/2016JD024882

[94] Georgiou G. K., Christoudias T., Proestos Y., Kushta J., Hadjinicolaou P., Lelieveld J. Air quality modelling in the summer over the eastern Mediterranean using WRF-Chem: chemistry and aerosol mechanism intercomparison. *Atmospheric Chemistry and Physics* 2018:18(3):1555–1571. doi.org/10.5194/acp-18-1555-2018

[95] The Royal Society. Geoengineering the climate: Science, governance and uncertainty. London: Royal Society, 2009.

**Gabriela Celeste Mulena.** In 2017, she received her Ph. D. degree in engineering from the National University of Cuyo (UNCuyo). As a doctoral student under mentorship of Dr. Enrique Puiafito, she focused her research on modelling of aerosol particles emission to mitigate extreme weather events (weather modification). She is currently a postdoctoral fellow in the Consejo Nacional de Investigaciones Científicas y Técnicas (CONICET), and works at Instituto Argentino de Nivología, Glaciología y Ciencias Ambientales (IANIGLA), in the City of Mendoza (Argentina). She has experience in numerical modeling at urban/regional scales using WRF and WRF/Chem, among other atmospheric modeling. As a postdoctoral researcher, she has focused her work on the influence of extreme weather events such as heat waves, temperature inversions and atmospheric stagnation episodes on the regional transport of pollutants in the Province of Mendoza, during the last 30 years.
ORCID ID: https://orcid.org/0000-0003-1945-4320

**Enrique Salvador Puliafito.** He received the Ph. D. degree in engineering (1989) from the University of Braunschweig (Germany) in the area of atmospheric physics. He has participated in research projects concerning stratospheric ozone and tropospheric water vapor. At present he is professor and researcher at the Universidad Tecnológica Nacional (UTN) of Mendoza (Argentina) where he leads a group in climate change research and air quality modelling and monitoring. Atmospheric numerical modelling use includes local scale: ISC3, AERMOD, and regional scale: HYSPLIT, WRF/CALMET/CALPUFF and WRF/Chem. Research member of Argentine Council for Science and Technology (CONICET). ORCID ID: https://orcid.org/0000-0001-9085-6870

**Susan Gabriela Lakkis.** She received the Ph. D. degree in Physics from University of Buenos Aires (UBA). Her skills and expertise are in topics related with atmospheric dynamics, clouds, meteorology and air quality. Currently, she is working at Universidad Tecnológica Nacional (UTN), Buenos Aires and Pontificia Universidad Católica de Argentina, Buenos Aires as a full-time researcher. Dr. Lakkis has published several papers in international journals some of the latter are: Adrián E. Yuchechen, S. Gabriela Lakkis & Pablo O. Canziani (2017), A seasonal climatology of UV reflectivity for southern South America, International Journal of Remote Sensing, 38:sup1, 28−56, DOI: 10.1080/01431161.2017.1388935; Adrián E. Yuchechen, S. Gabriela Lakkis & Pablo O. Canziani (2017); Linear and Non-Linear Trends for Seasonal $NO_2$ and $SO_2$ Concentrations in the Southern Hemisphere (2004−2016) Remote Sens. 2017, 9(9), 891; doi:10.3390/rs9090891. She also has strongly cooperated in several Scientific Assessment of Ozone. ORCID ID: https://orcid.org/0000-0001-7562-8204